

## Remnant Fermi Surfaces in Photoemission

C. Kusko\* and R. S. Markiewicz

*Physics Department and Barnett Institute, Northeastern University, Boston, Massachusetts 02115*

(Received 24 March 1999)

Recent experiments have introduced a new concept for analyzing the photoemission spectra of correlated electrons—the remnant Fermi surface (rFs), which can be measured even in systems which lack a conventional Fermi surface. Here, we analyze the rFs in a number of interacting electron models, and find that the results fall into two classes. For systems with particle-particle (pairing) instabilities, the rFs is an accurate replica of the true Fermi surface. In the presence of particle-hole (nesting) instabilities, the rFs is a map of the resulting superlattice Brillouin zone. The results suggest that the gap in  $\text{Ca}_2\text{CuO}_2\text{Cl}_2$  is of particle-hole origin.

PACS numbers: 71.18.+y, 71.27.+a, 79.60.-i

Recently, a new experimental tool has been introduced [1] to parametrize photoemission (PE) data in strongly correlated metals: the “remnant Fermi surface” (rFs). This is the locus of points in  $\vec{k}$  space where the PE intensity associated with a particular quasiparticle peak falls to half of its peak value. For an ordinary metal, these points would correspond to the Fermi surface, but in strongly correlated metals the points do not necessarily fall at the same energy—the rFs may display a considerable dispersion.

Ronning *et al.* [1] measured the rFs of  $\text{Ca}_2\text{CuO}_2\text{Cl}_2$  (CCOC), a half filled Mott insulator, and compared it with the rFs of optimally doped  $\text{Bi}_2\text{Sr}_2\text{CaCu}_2\text{O}_8$  (BSCCO). When underdoped, the dispersion of the pseudogap in BSCCO evolves toward that of CCOC [2], suggesting a close connection between CCOC and the pseudogap in BSCCO (or at least the “hump” feature in the dispersion [3]). Qualitatively, the rFs of CCOC seems consistent with Luttinger’s theorem, even though it displays a considerable dispersion. Despite this, the rFs’s of the two materials are strikingly different, and cannot evolve from each other via rigid band filling (they cross). A proper understanding of the rFs could lead to an improved model for the pseudogap in these materials.

In this Letter we analyze the rFs expected for a variety of interacting electron systems, and show that they do not necessarily provide information about the Fermi surface. The results fall into two classes, depending on whether the interaction can be characterized as “nesting” or “pairing.” Only in the latter case is the rFs a reliable map of the Fermi surface. In the former case, it maps out the superlattice Brillouin zone generated by the nesting instability.

A number of different mechanisms have been proposed for the origin of pseudogaps in the cuprates. These include magnetic (spin density wave—SDW) [4], flux phase (RVB) [5–8], charge ordering (CDW) [7,9], and superconducting fluctuations [10]. These instabilities fall into two classes: the first three are instabilities of the particle-hole ( $p$ - $h$ ) propagator (here called  $p$ - $h$  or generalized nesting instabilities) associated with a preferred *nesting* vector, here  $\vec{Q} = (\pi, \pi)$ , while the last is a particle-particle ( $p$ - $p$ )

instability, a *pairing* instability in the uniform susceptibility at  $\vec{q} = 0$ . The  $p$ - $h$  instabilities include both conventional nesting instabilities (CDW and SDW) at weak coupling and the Mott instability at strong coupling [11]. We find that the rFs has two strikingly different origins in these two classes, but there is relatively little variation within a given class. In CCOC the rFs seems to indicate the locus of the reduced Brillouin zone, characteristic of a  $p$ - $h$  instability.

An important sum rule relating the integrated intensity to the momentum distribution has been utilized by Randeria *et al.* [12] for analyzing angle-resolved photoemission spectroscopy (ARPES) data, and is given by

$$n(\vec{k}) = \int_{-\infty}^{\infty} d\omega f(\omega) A(\vec{k}, \omega), \quad (1)$$

where  $A(\vec{k}, \omega)$  is the one particle spectral function of the model,  $n(\vec{k}) = \langle c_{\vec{k}}^\dagger c_{\vec{k}} \rangle$  is the momentum distribution, and  $f(\omega)$  is the Fermi function. Although  $n(\vec{k})$  is a ground state property, they proved that in the limit of the sudden approximation the frequency integrated spectral function gives the momentum distribution. They employed this sum rule to determine the momentum distribution in BSSCO and YBCO. Ronning *et al.* [1] extended this methodology to strongly correlated electron compounds. By defining  $k_F$  as the point of steepest descent, they showed that even when strong Coulomb correlations destroy the Fermi-liquid character of the system,  $n(\vec{k})$  still drops sharply, allowing the determination of a rFs.

In the following, we calculate the spectral function  $A(\vec{k}, \omega)$  and the momentum distribution for mean-field models with a variety of instabilities. Figure 1 illustrates the rFs’s associated with SDW instabilities for a variety of superlattices. The energy dispersion has the standard one-band form

$$e_{\vec{k}} = -2t_0(\cos k_x a + \cos k_y a) - 4t_1 \cos k_x a \cos k_y a, \quad (2)$$

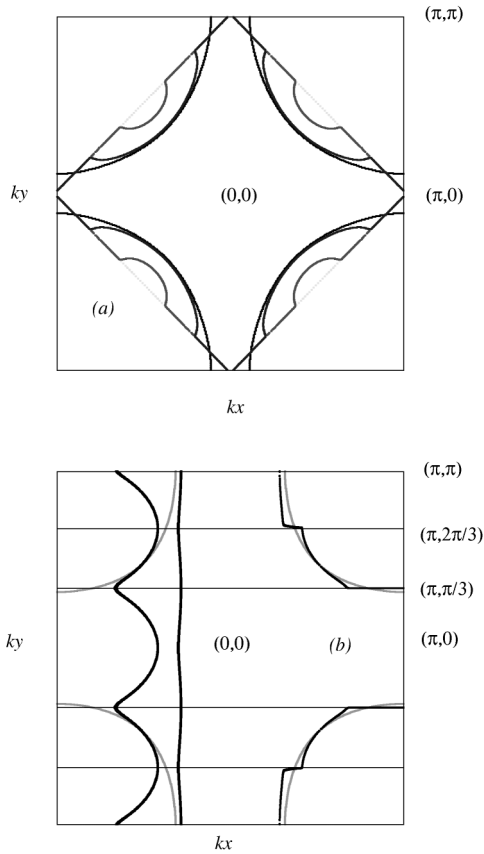


FIG. 1. Remnant Fermi surfaces for SDW instabilities with different nesting vectors at  $T = 0$  K. (a) Evolution of the rFs toward a perfect square with increasing SDW gap, for nesting vector  $\vec{Q} = (\pi, \pi)$ ; (from darkest to lightest)  $O_{SDW} = 0, 100, 300, 500$  meV. (b) Fermi and remnant Fermi surface for an SDW with the nesting vector  $\vec{Q}' = (0, \frac{2\pi}{3})$ ; left = Fermi surfaces without nesting (grey) and with nesting  $O_{SDW} = 100$  meV (black), right = the rFs. The horizontal parts of the rFs map the superlattice boundaries (light lines).

with  $t_0 = 0.25$  eV,  $t_1 = -0.45t_0$ . While the present calculations are for an SDW, the rFs's for a CDW are identical [13], while those for a flux phase are very similar [14]: over part of the surface, there is no gap, and the rFs is dispersionless, coinciding with the Fermi surface at  $e_{\vec{k}} = E_F$ ; here  $n(\vec{k}) = 1/2$  is mainly due to the Fermi function in Eq. (1). Over the rest of the zone, the rFs lies along the zone boundaries of the nesting superlattice. On this part of the rFs there is considerable dispersion, and  $n(\vec{k}) = 1/2$  due to the coherence factor, discussed below. Note the presence in the rFs of “half pockets.” The Fermi surface for a doped antiferromagnet is a full pocket. However, because of the coherence factors the “ghost” Fermi surface—the half of the pocket beyond the magnetic line  $(\pi, 0)$ - $(0, \pi)$ —always has a weight less than one-half, and hence is not present in the rFs. Therefore the rFs lies in the reduced Brillouin zone. By contrast, the rFs for a  $p$ - $p$  (pairing) instability is always located below  $E_F$  at the superconducting gap, dispersionless for  $s$ -wave, dispersive for  $d$ -wave, but in both cases faithfully following the con-

tours of the Fermi surface. In Fig. 1a one can see that in the strong coupling regime a large  $p$ - $h$  instability causes the rFs to follow the antiferromagnetic Brillouin zone even if nesting is poor.

In Fig. 1a, we consider nesting between the saddle points  $(\pi, 0)$  and  $(0, \pi)$  leading to a rFs mapping of the magnetic  $\sqrt{2} \times \sqrt{2}$  superlattice. This is the superlattice most likely to be relevant near half filling in the cuprates, and indeed matches the rFs found by Ronning *et al.* [1] in CCOC. We can, however, extend this procedure for an arbitrary nesting vector. In Fig. 1b the band parameters are chosen such that segments of the Fermi surface (grey line) are approximately nested by a vector  $\vec{Q}' = (0, 2\pi/3)$ . When the interaction is turned on new superlattice boundaries form (thin horizontal lines), and the rFs is again composed of zone boundaries and Fermi surface fragments (right, dark lines). The new Fermi surfaces are redrawn on the left in an extended zone scheme (black lines). This example shows that the rFs should be applicable to a wide variety of structural instabilities. Moreover, in the high- $T_c$  cuprates, it has been proposed that the incommensurate neutron scattering peaks [15,16] are associated with nesting (i.e.,  $p$ - $h$ ) instabilities.

If the pseudogap is due to a  $p$ - $h$  instability competing with superconductivity, there should be a characteristic evolution of the rFs with doping, from nestinglike at half filling to pairinglike in the overdoped regime. The phase diagram has been worked out for such a competition, both for CDW-to- $s$ -wave superconductivity [13] and for flux phase to  $d$ -wave [8,14]. In both cases, we find the evolution of the rFs's is nearly identical. Figure 2 illustrates this evolution for the latter case. Note that since the phase at half filling is fully gapped (a Mott insulator), the rFs is perfectly square. The two limiting cases, insulator and optimally doped, bear a marked resemblance to the experimental observations [1].

In the calculations of Fig. 2, we took the competing phases to be  $d$ -wave superconductivity, with gap  $\Delta_k^d = \Delta^d \gamma_{\vec{k}}$ , with  $\gamma_{\vec{k}} = \cos k_x a - \cos k_y a$  and an orbital antiferromagnet [17,18], a  $ph$ - $h$  instability with gap  $O_k^{JC} = O^{JC} \gamma_{\vec{k}}$ , which is essentially equivalent to the flux phase instability introduced by Affleck and Marston [19]. We consider a one-band model, Eq. (2), with correlation effects simulated by a doping dependent  $t_0 = xt_0^*$ ,  $t_0^* = 2.3$  eV, and the Van Hove singularity (VHS) pinned close to the Fermi level over an extended range of doping [7,13].

The mean-field quasiparticle dispersion is

$$E_{\pm, \vec{k}}^2 = \frac{1}{2} [\epsilon_{\vec{k}}^2 + \epsilon_{\vec{k}+\vec{Q}}^2 + 2\Delta_k^2 + 2O_k^{JC2} \pm (\epsilon_{\vec{k}} + \epsilon_{\vec{k}+\vec{Q}}) \hat{E}_{\vec{k}}], \quad (3)$$

with  $\hat{E}_{\vec{k}} = \sqrt{(\epsilon_{\vec{k}} - \epsilon_{\vec{k}+\vec{Q}})^2 + 4O_k^{JC2}}$ . The above calculation differs from that of Fig. 1, in that the shape of the Fermi surface evolves with doping. However, the evolution of the rFs for the flux phase gap is generically toward

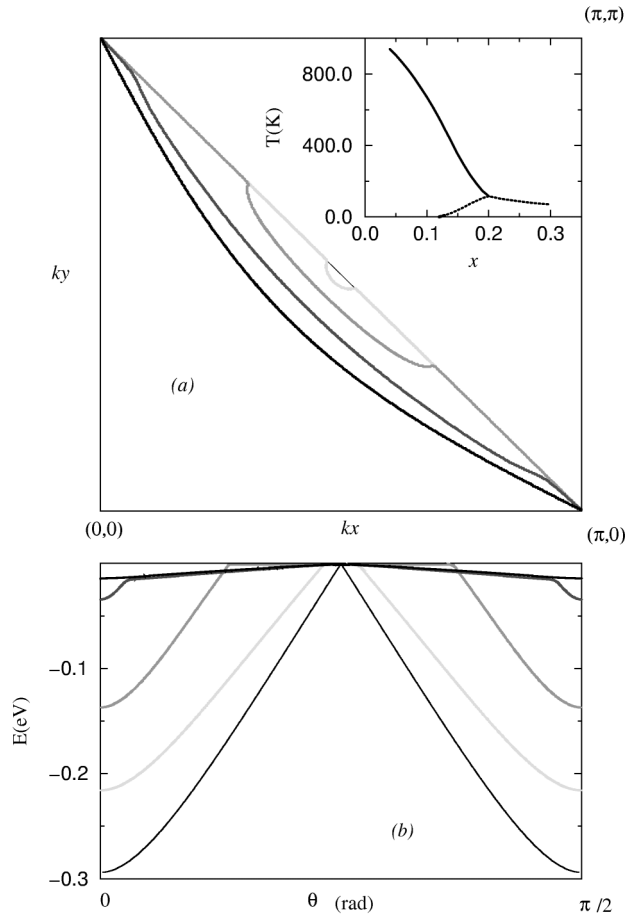


FIG. 2. (a) Evolution of the rFs from half filling to optimal doping at  $T = 0$  K with self-consistent gap parameters for a model with  $d$ -wave superconductivity and flux phase. Curves from lightest to darkest:  $x = 0$  (thin line), 0.04, 0.1, 0.19, and 0.26 (black line). Inset: Pseudogap phase diagram. Solid line = pseudogap transition  $T^*$ ; dotted line = superconducting transition  $T_c$ . (b) Quasiparticle dispersion along the rFs plotted in (a),  $\tan\theta = k_x/k_y$ .

a square Fermi surface at half filling (thin line in Fig. 2). For finite doping, only part of the Fermi surface is gapped, and the rFs has two parts, a (hole pocket) Fermi surface on the ungapped part of the rFs, and a segment of square on the gapped part. With increasing gap magnitude, the former feature shrinks and the latter grows, until the full Fermi surface is gapped and the rFs is square. There is considerable dispersion of the rFs (Fig. 2b), since the flux phase gap vanishes when  $k_x = k_y$ . The shrinking of the Fermi surface is reminiscent of the evolution in BSCCO reported by Norman *et al.* [20]. It should be noted that the rFs is not equivalent to the minimum gap locus introduced by Ding *et al.* [21].

The origin of the rFs can be understood from these calculations. In the competing flux phase- $d$ -wave model,  $n(\vec{k})$  can be written as

$$n(k) = \frac{1}{2} \left( 1 - \cos^2\phi \cos 2\phi_+ \tanh \frac{\beta E_{+\vec{k}}}{2} - \sin^2\phi \cos 2\phi_- \tanh \frac{\beta E_{-\vec{k}}}{2} \right), \quad (4)$$

with  $\tan 2\phi_{\pm} = 2\Delta_{\vec{k}}/(\epsilon_{\vec{k}} + \epsilon_{\vec{k}+\vec{Q}} \pm \hat{E}_{\vec{k}})$  and  $\tan 2\phi = 2O_{\vec{k}}^{\text{JC}}/(\epsilon_{\vec{k}} - \epsilon_{\vec{k}+\vec{Q}})$ . For a pure  $d$ -wave superconductivity model this becomes

$$n(k) = \frac{1}{2} \left( 1 - \frac{\epsilon_{\vec{k}}}{E_{\vec{k}}} \tanh \frac{\beta E_{\vec{k}}}{2} \right), \quad (5)$$

with  $E_{\vec{k}} = \sqrt{\epsilon_{\vec{k}}^2 + \Delta_{\vec{k}}^2}$ , showing that the rFs coincides with the true Fermi surface:  $n(\vec{k}) = 1/2$  when  $\epsilon_{\vec{k}} = 0$ . For a pure magnetic (or charge) instability model  $n(\vec{k})$  is given by

$$n(\vec{k}) = \frac{1}{2} \left( 1 - \cos^2\phi \tanh \frac{\beta E_{+\vec{k}}^{\text{nest}}}{2} - \sin^2\phi \tanh \frac{\beta E_{-\vec{k}}^{\text{nest}}}{2} \right), \quad (6)$$

with  $E_{\pm\vec{k}}^{\text{nest}} = (\epsilon_{\vec{k}} + \epsilon_{\vec{k}+\vec{Q}} \pm \hat{E}_{\vec{k}})/2$ . As  $T \rightarrow 0$ , the two  $\tanh$ 's go to 1 or  $-1$ , so  $n(\vec{k}) = 1/2$  when  $\cos^2\phi - \sin^2\phi = 0$ , or, from the definition of  $\phi$  [below Eq. (4)],  $\epsilon_{\vec{k}} = \epsilon_{\vec{k}+\vec{Q}}$ . For the present model, this is the superlattice Brillouin zone boundary.

In the above calculation, the reduction  $n(k) < 1$  can be traced to a coherence factor coupling two bare states. This should be contrasted with the insulator gap due to a filled band [22]. In the latter case, there is no coherence factor, and  $n(k) = 1$  for all filled states.

In the underdoped regime, as temperature is lowered the cuprates pass first into the pseudogap phase, at temperature  $T^*$ , then into a superconducting phase at  $T_c$  (inset, Fig. 2a). In the present scenario,  $T^*$  would signal a transition to a  $p$ - $h$  phase with a gap (or pseudogap if realistic fluctuations are included [4,23]), leaving hole pockets behind. Below  $T_c$ , an additional,  $p$ - $p$  gap opens at the hole pockets. However, a careful look at the rFs shows a more complicated evolution, Fig. 3a: the shape of the hole pockets changes, with an accompanying transfer of spectral weight from the nesting to the pairing parts of the rFs. Note that in Fig. 3a the rFs has the same locus in  $k$  space as the true hole pocket Fermi surface above  $T_c$ , but from Fig. 3b there is a dramatic shift in dispersion of this rFs as the superconducting gap opens.

In comparing these results to experiment, the rFs of CCOC clearly displays the square shape expected for a predominantly  $p$ - $h$  interaction. This is consistent with all of the pseudogap models noted above, except for preformed pairs. In fact, preformed pairs would still be a possibility, if strong correlation effects renormalized the (true) Fermi surface to square at half filling. Such renormalization has been proposed previously [24]. However, in these theories, the renormalization leads to greatly enhanced nesting, and is less favorable for pairing. The most likely conclusion is that the pseudogap in the underdoped cuprates represents some magnetic (or charge) instability, which is fundamentally competing with superconductivity; this is consistent [13] with recent experimental evidence for mixed behavior of the gap [25]. Clearly, since the cuprates

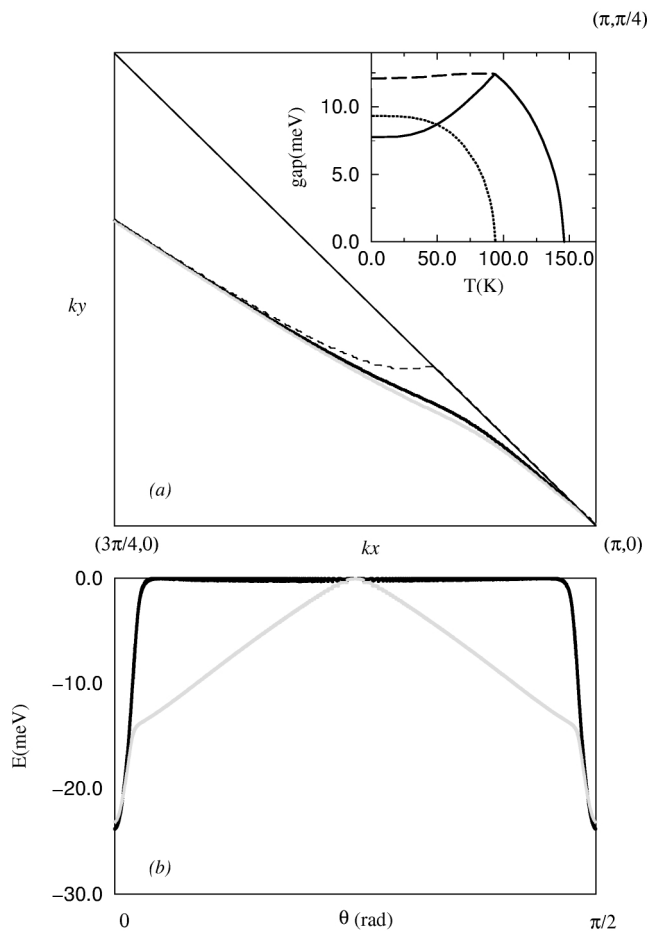


FIG. 3. (a) Evolution of the rFs with temperature for a fixed doping  $x = 0.19$ : black line— $T = 0$  K; grey line— $T = T_c = 94$  K ( $\Delta^d = 0$  meV); dashed line shows what the flux phase rFs at  $T = 0$  K would be if  $\Delta^d = 0$  meV. Inset: Temperature dependence of the superconducting and flux phase gaps; dotted line =  $\Delta^d$ ; solid line =  $O^{JC}$ ; dashed line =  $\sqrt{\Delta^d{}^2 + O^{JC}{}^2}$ . (b) Quasiparticle dispersion along the rFs plotted in (a).

are quasi-two-dimensional, there should be prominent superconducting fluctuations above  $T_c$ , but they do not represent the dominant part of the pseudogap.

Some results on rFs's have already appeared in the literature. Friedel and Peter [26] discussed the effect of CDW and SDW gaps on Fermi surfaces determined by positron annihilation, while Bulut *et al.* [11] discussed the role of coherence factors on SDW rFs's. The present paper stresses the great generality of the phenomenon, and its use in distinguishing nesting from pairing phenomena. While the rFs should play an important role in future ARPES studies, its full potential must await a more complete understanding of the pseudogap phenomenon.

The present results suggest a number of experimental tests. The rFs should be mapped out in the cuprates as a

function of doping. In particular, the results of Norman *et al.* [20] should be extended to the full rFs. Observation of a shift in spectral weight with temperature, Fig. 3 would provide strong additional evidence that the pseudogap is a  $p$ - $h$  (nesting) phenomenon, and not due to preformed pairs. Moreover, the rFs can be studied in other systems, to confirm the predicted properties. A start has already been made in CDW systems [27]. Other Mott insulators would also be of interest, particularly nonmagnetic Mott insulators.

\*On leave of absence from Institute of Atomic Physics, Bucharest, Romania.

- [1] F. Ronning *et al.*, *Science* **282**, 2067 (1998).
- [2] R. B. Laughlin, *Phys. Rev. Lett.* **79**, 1726 (1997).
- [3] J. C. Campuzano *et al.*, *cond-mat/9906335*.
- [4] A. P. Kampf and J. R. Schrieffer, *Phys. Rev. B* **41**, 6399 (1990); **42**, 7967 (1990).
- [5] R. B. Laughlin, *J. Phys. Chem. Solids* **56**, 1627 (1995).
- [6] X.-G. Wen and P. A. Lee, *Phys. Rev. Lett.* **76**, 503 (1996).
- [7] R. S. Markiewicz, *Phys. Rev. B* **56**, 9091 (1997).
- [8] E. Cappelluti and R. Zeyher, *Physica (Amsterdam)* **312C**, 313 (1999); *Phys. Rev. B* **59**, 6475 (1999).
- [9] R. A. Klemm (unpublished).
- [10] V. J. Emery and S. A. Kivelson, *Nature (London)* **374**, 434 (1995); M. Randeria, *cond-mat/9710223* (unpublished); Q. Chen, I. Kosztin, B. Jankó, and K. Levin, *Phys. Rev. Lett.* **81**, 4708 (1998).
- [11] N. Bulut, D. J. Scalapino, and S. R. White, *Phys. Rev. Lett.* **73**, 748 (1994).
- [12] M. Randeria *et al.*, *Phys. Rev. Lett.* **74**, 4951 (1995).
- [13] R. S. Markiewicz, C. Kusko, and V. Kidambi, *Phys. Rev. B* **60**, 627 (1999).
- [14] C. Kusko and R. S. Markiewicz (unpublished).
- [15] K. Yamada *et al.*, *Phys. Rev. B* **57**, 6165 (1998).
- [16] H. A. Mook *et al.*, *Nature (London)* **395**, 580 (1998).
- [17] H. J. Schulz, *Phys. Rev. B* **39**, 2940 (1989).
- [18] R. S. Markiewicz and M. T. Vaughn, *J. Phys. Chem. Solids* **59**, 1737 (1998); *Phys. Rev. B* **57**, 14052 (1998).
- [19] I. Affleck and J. B. Marston, *Phys. Rev. B* **37**, 3774 (1988).
- [20] M. R. Norman *et al.*, *Nature (London)* **392**, 158 (1998).
- [21] H. Ding *et al.*, *Phys. Rev. Lett.* **78**, 2628 (1997).
- [22] J. M. Ziman, *Principles of the Theory of Solids* (Cambridge University Press, Cambridge, 1964), p. 340.
- [23] R. S. Markiewicz, *Physica (Amsterdam)* **169C**, 63 (1990).
- [24] R. S. Markiewicz, *J. Phys. Chem. Solids* **58**, 1179 (1997) (see p. 1223); N. Furukawa, T. M. Rice, and M. Salmhofer, *Phys. Rev. Lett.* **81**, 3195 (1998).
- [25] C. Panagopoulos and Tao Xiang, *Phys. Rev. Lett.* **81**, 2336 (1998).
- [26] J. Friedel and M. Peter, *Europhys. Lett.* **8**, 79 (1989).
- [27] Th. Pillo *et al.*, *cond-mat/9902327*.